



Novel brain permeant mTORC1/2 inhibitors are as efficacious as rapamycin or everolimus in mouse models of acquired partial epilepsy and tuberous sclerosis complex

Wiebke Theilmann^{a,1}, Birthe Gericke^{a,b,1}, Alina Schidlitzki^{a,1}, Syed Muhammad Muneeb Anjum^{a,2}, Saskia Borsdorf^a, Timon Harries^a, Steven L. Roberds^c, Dean J. Aguiar^c, Daniela Brunner^d, Steven C. Leiser^d, Dekun Song^d, Dorian Fabbro^e, Petra Hillmann^e, Matthias P. Wymann^f, Wolfgang Löscher^{a,b,*}

^a Department of Pharmacology, Toxicology, and Pharmacy, University of Veterinary Medicine Hannover, Germany

^b Center for Systems Neuroscience, Hannover, Germany

^c Tuberous Sclerosis Alliance, Silver Spring, MD, USA

^d PsychoGenics, Paramus, NJ, USA

^e PIQUR Therapeutics AG, Basel, Switzerland

^f Department of Biomedicine, University of Basel, Mattenstrasse 28, 4058, Basel, Switzerland

ARTICLE INFO

Keywords:

Acquired epilepsies
Genetic epilepsies
Antiseizure drugs
TORopathies
Tolerability

ABSTRACT

Mechanistic target of rapamycin (mTOR) regulates cell proliferation, growth and survival, and is activated in cancer and neurological disorders, including epilepsy. The rapamycin derivative (“rapalog”) everolimus, which allosterically inhibits the mTOR pathway, is approved for the treatment of partial epilepsy with spontaneous recurrent seizures (SRS) in individuals with tuberous sclerosis complex (TSC). In contrast to the efficacy in TSC, the efficacy of rapalogs on SRS in other types of epilepsy is equivocal. Furthermore, rapalogs only poorly penetrate into the brain and are associated with peripheral adverse effects, which may compromise their therapeutic efficacy. Here we compare the antiseizure efficacy of two novel, brain-permeable ATP-competitive and selective mTORC1/2 inhibitors, PQR620 and PQR626, and the selective dual pan-PI3K/mTORC1/2 inhibitor PQR530 in two mouse models of chronic epilepsy with SRS, the intrahippocampal kainate (IHK) mouse model of acquired temporal lobe epilepsy and *Tsc1*^{GFAP} CKO mice, a well-characterized mouse model of epilepsy in TSC. During prolonged treatment of IHK mice with rapamycin, everolimus, PQR620, PQR626, or PQR530; only PQR620 exerted a transient antiseizure effect on SRS, at well tolerated doses whereas the other compounds were ineffective. In contrast, all of the examined compounds markedly suppressed SRS in *Tsc1*^{GFAP} CKO mice during chronic treatment at well tolerated doses. Thus, against our expectation, no clear differences in antiseizure efficacy were found across the three classes of mTOR inhibitors examined in mouse models of genetic and acquired epilepsies. The main advantage of the novel 1,3,5-triazine derivatives is their excellent tolerability compared to rapalogs, which would favor their development as new therapies for TORopathies such as TSC.

Abbreviations: BBB, blood-brain barrier; CKO, conditional knockout; EEG, electroencephalogram; HPD, hippocampal paroxysmal discharge; HVSWS, high-voltage spike wave; IHK, intrahippocampal kainate; mTOR, mechanistic target of rapamycin; PEG, polyethylene glycol; PI3K, phosphoinositide 3-kinase; PKB, protein kinase B; PND, postnatal day; SE, status epilepticus; SBEDD, sulfolbutyl-ether-β-cyclodextrin; SEGA, subependymal giant cell astrocytoma; SRS, spontaneous recurrent seizures; TLE, temporal lobe epilepsy; TSC, tuberous sclerosis complex.

* Corresponding author. Department of Pharmacology, Toxicology and Pharmacy, University of Veterinary Medicine, Bünteweg 17, D-30559, Hannover, Germany.

E-mail address: wolfgang.loescher@tiho-hannover.de (W. Löscher).

¹ These authors contributed equally to this study.

² Present address Institute of Pharmaceutical Sciences, University of Veterinary & Animal Sciences, Lahore, Pakistan.

<https://doi.org/10.1016/j.neuropharm.2020.108297>

Received 17 June 2020; Received in revised form 27 August 2020; Accepted 1 September 2020

Available online 3 September 2020

0028-3908/© 2020 Elsevier Ltd. All rights reserved.

1. Introduction

Current epilepsy therapies are primarily symptomatic and target ion channels or neurotransmitters involved in seizure generation and spread. Yet these drugs also modulate normal brain functions, resulting in respective adverse effects (Rogawski et al., 2016). In addition, at least one third of epilepsy patients do not respond to current antiseizure medications (Devinsky et al., 2018). Epilepsies are complex and heterogeneous disorders, so more recently developed etiology-specific therapies are thought to possess significant advantages over previous, less specific treatments (Devinsky et al., 2018). Indeed, epilepsy was among the first disease areas that began applying principles of precision medicine to its treatment (Leach, 2018). One of the most important examples of etiology-specific therapy of epilepsy is treatment of patients with tuberous sclerosis complex (TSC) with everolimus, a drug that allosterically inhibits the mechanistic target of rapamycin (mTOR) pathway (Ostendorf and Wong, 2015). TSC is caused by mutations in the *TSC1* or *TSC2* genes, which result in dysregulation of the phosphoinositide 3-kinase (PI3K)/protein kinase B (PKB/Akt)/mTOR (PI3K/Akt/mTOR) signaling pathway and a clinical manifestations characterized by hamartomas throughout the body, cortical malformations (known as tubers), subependymal giant cell astrocytomas (SEGAs) and medically intractable epilepsy (Jeong and Wong, 2015). Everolimus is approved for the treatment of SEGAs, kidney tumors, and partial epilepsy in individuals with TSC (Lechuga and Franz, 2019). Because of its immunosuppressant activity its use may, however, be associated with adverse effects, which prevent prolonged chronic treatment in some individuals (Franz et al., 2016).

Other genetic epilepsies caused by disrupted mTOR activity (“TORopathies”) include PTEN hamartoma syndrome and focal cortical dysplasia, which is the most common cause of medically refractory epilepsy in the pediatric population, but mTOR hyperactivation has also been described in the brains of humans with acquired focal epilepsies (Jeong and Wong, 2015; Ostendorf and Wong, 2015; Griffith and Wong, 2018). Furthermore, mTOR activation has been shown to occur in animal models of acquired epilepsy, for example following traumatic brain injury, neonatal hypoxia, or status epilepticus (SE) induced by pilocarpine or kainate (Galanopoulou et al., 2012; Wong, 2013; Citraro et al., 2016). In such models, mTOR activation leads to mossy fiber sprouting, neuronal death, and neurogenesis, which may promote epileptogenesis (Citraro et al., 2016; Godale and Danzer, 2018). Thus, inhibiting mTOR has been suggested both as late symptomatic treatment of seizures or early preventative therapy in patients at risk of developing epilepsy (Vezzani, 2012; Jeong and Wong, 2015; Ostendorf and Wong, 2015; Griffith and Wong, 2018). Whereas there is convincing evidence in mouse models of TSC for antiseizure (antiepileptic) and anti-epileptogenic (epilepsy-preventing) efficacy of mTOR inhibitors, data from models of acquired epilepsies are instead equivocal (Galanopoulou et al., 2012; Wong, 2013; Citraro et al., 2016; Jozwiak et al., 2020). Furthermore, most published experimental studies in animal models of epilepsy used rapamycin (sirolimus) despite the fact that everolimus is the only mTOR inhibitor approved for epilepsy treatment and has higher bioavailability and a higher potency to deplete mTOR complex 2 (mTORC2) signaling in the long term, as compared to rapamycin (Klawitter et al., 2015). As a consequence of TORC1 inhibition by rapamycin and related compounds (“rapalogs”), class IA PI3Ks are over-activated by the loss of a negative feedback loop, resulting in a PI3K/TORC2-dependent increase in PKB/Akt activity, which may compromise the therapeutic efficacy of rapamycin in seizure disorders (Laplante and Sabatini, 2012). Compounds targeting the catalytic site of both TORC1 and TORC2 are therefore expected to provide a more efficient block of signaling downstream of PI3K (Hassan et al., 2014; Chiarini et al., 2015; Janku et al., 2018; Hillmann and Fabbro, 2019).

In the present study, we compared the efficacy of the allosteric mTOR inhibitors rapamycin and everolimus to suppress spontaneous recurrent seizures (SRS) in the intrahippocampal kainate (IHK) mouse

model of temporal lobe epilepsy (TLE), a widely used model of acquired focal epilepsy (Henshall, 2017; Duveau and Roucard, 2017). As mentioned above, mTOR hyperactivity has been reported previously for this model, but rapamycin or more effective novel catalytic inhibitors of the PI3K/Akt/mTOR pathway were not capable of preventing epilepsy (Shima et al., 2015; Gericke et al., 2020). These novel catalytic (ATP-competitive) inhibitors, i.e., the mTORC1/2 inhibitor PQR620 (Rageot et al., 2018) and the dual pan-PI3K/mTORC1/2 inhibitor PQR530 (Rageot et al., 2019, Fig. 1) were also included in the present study. We have shown recently that these two compounds exhibit a much better brain permeability and tolerability than rapamycin and everolimus (Brandt et al., 2018; Rageot et al., 2018, 2019; Gericke et al., 2020). In addition, we included the novel brain-penetrant catalytic mTORC1/C2 inhibitor PQR626 (Fig. 1), which has been optimized for systemic stability in humans (Borsari et al., 2020). For comparison with the efficacy of the allosteric and catalytic mTOR and PI3K/mTOR inhibitors in the kainate model of acquired epilepsy, respective efficacy in a mouse TSC model was evaluated. Our hypothesis was, based on the more complete inhibition of the hyperactive PI3K/Akt/mTOR pathway, that the catalytic inhibitors PQR530, PQR620 and PQR626 would be more effective to suppress SRS than the allosteric inhibitors rapamycin and everolimus.

2. Materials and methods

2.1. Animals

For the intrahippocampal kainate (IHK) mouse model, male CD-1 mice were obtained from Charles River (Sulzfeld, Germany) at an age of 7 weeks. Similar to NMRI mice (which we used previously for the IHK model), CD-1 is a Swiss strain-derived multipurpose mouse outbred strain (Chia et al., 2005), which is widely used in epilepsy research (Löscher et al., 2017). Animals were housed under controlled conditions (ambient temperature 22–24 °C, humidity 30–50%, lights on from 6:00 a.m. to 6:00 p.m.). Food and water were provided *ad libitum*. Mice were adapted to the laboratory conditions for at least one week before used in experiments. Experiments were performed according to the EU council directive 2010/63/EU and the German Law on Animal Protection (“Tierschutzgesetz”). Ethical approval for the study was granted by an ethical committee (according to §15 of the Tierschutzgesetz) and the governmental agency (Lower Saxony State Office for Consumer Protection and Food Safety; LAVES) responsible for approval of animal experiments in Lower Saxony (reference number for this project: 14/1659). All efforts were made to minimize both the suffering and the number of animals. All animal experiments of this study are reported in accordance with ARRIVE guidelines (Kilkenny et al., 2010).

For the TSC mouse model, *Tsc1*^{flx/flx}-GFAP-Cre knockout (*Tsc1*^{GFAP}CKO) mice of either sex with conditional inactivation of the *Tsc1* gene were bred at PsychoGenics using breeding pairs obtained from Michael Wong’s Laboratory (Washington University, St. Louis, MO) to generate a knockout of *Tsc1* in glial fibrillary acidic protein (GFAP)-expressing cells (Uhlmann et al., 2002). All mice were handled according to the PsychoGenics ethical guidelines. Light/dark cycles were maintained at 12 h/12 h, temperature was 20–23 °C, and humidity ~50%. Food and water were provided *ad libitum*. Assessment and approval of the study was obtained by the Association for Assessment and Accreditation of Laboratory Animal Care (approval IACUC 282_0616).

2.2. Intrahippocampal kainate (IHK) mouse model

In this model, SE is induced by unilateral injection of kainate into the CA1 sector of the dorsal hippocampus (Suzuki et al., 1995; Bouillier et al., 1999). For this purpose, CD-1 mice were anesthetized with chloral hydrate (500 mg/kg i.p.) and kainate monohydrate (0.21 µg in 50 nl saline) was stereotaxically injected into the right CA1 area of the dorsal hippocampus as described previously (Twele et al., 2016a). Stereotaxic coordinates (in mm from bregma) were AP, −2.2; LL, −1.7; DV, −1.4,

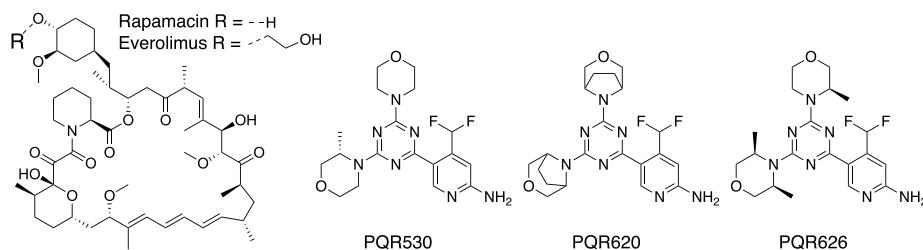


Fig. 1. Structures of rapalogs (rapamycin, everolimus) and novel catalytic (ATP-competitive) inhibitors of mTORC1/C2 (PQR620, PQR626) and PI3K/mTORC1/C2 (PQR530).

using the mouse brain atlas of Paxinos and Franklin (2012). The correct location of the injection was confirmed in separate mice of the cohorts used for the present experiments, and coordinates were adapted if needed. Kainate was slowly injected over 60 s with a 0.5 μ l micro-syringe. After injection of kainate, the needle of the syringe was maintained in situ for additional 2 min to limit reflux along the injection track. For EEG recordings, the animals were immediately implanted with bipolar electrodes aimed at the site of kainate injection in the ipsilateral CA1, using the same coordinates as for kainate injection (see Twele et al., 2016a). A screw, placed above the left parietal cortex, served as the indifferent ground electrode. Additional skull screws, superglue (Pattex® Ultra Gel; Henkel, Düsseldorf, Germany), and dental acrylic cement (Paladur®; Kulzer GmbH; Hanau, Germany) anchored the entire headset. During all surgical procedures and for about 1 h thereafter mice were kept on a warming pad to avoid hypothermia.

Furthermore, mice received electrolyte/glucose solution (Sterofundin® VG-5; B. Braun Melsungen AG; Melsungen, Germany) subcutaneously to compensate for loss of fluid and food during the day of surgery. Video/EEG monitoring was used to verify that kainate induced an SE. Furthermore, starting about 6 weeks after kainate, continuous video/EEG monitoring over 4 days was used for analysis of SRS (Fig. 2A). Only mice with frequent electrographic SRS (≥ 3 /h) were used for drug studies, which started about 8 weeks after kainate.

For EEG-recording, mice were connected via a flexible cable to a system consisting of 4 one-channel bioamplifiers (ADInstruments Ltd., Sydney, Australia) and analog-digital converters (PowerLab 8/30 ML870 or PowerLab 4/35 PL3504/P, ADInstruments). The data were recorded (sampling rate 200 Hz, time constant 0.1 s, low pass filter of >60 Hz, 50 Hz notch filter) and analyzed with LabChart 8 for Windows software (ADInstruments). The EEG-recording was directly linked to

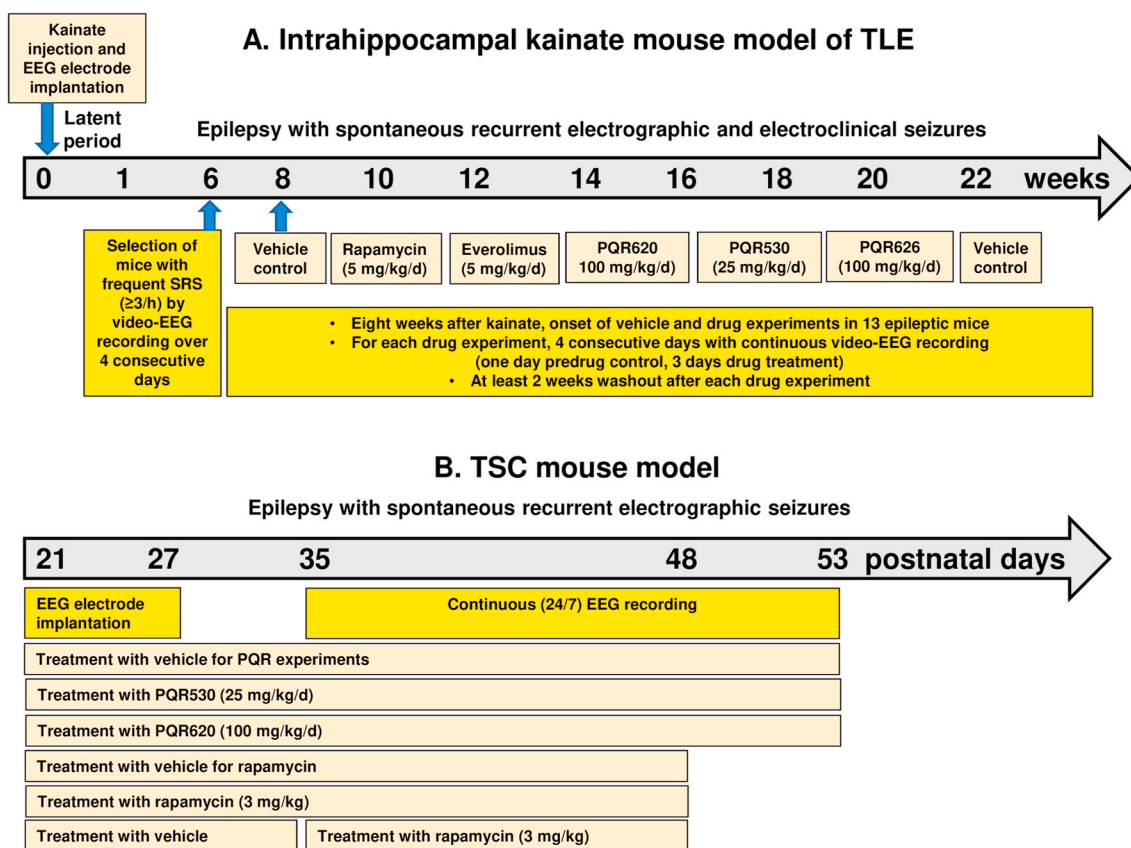


Fig. 2. Schematic illustration of the experimental design of the drug experiments performed in this study in two mouse models of epilepsy. A: In the intra-hippocampal kainate mouse model of TLE, kainate was injected in CD-1 mice at an age of about 8 weeks (indicated by “0”). The experiments were performed in two cohorts, of which a total of 13 CD-1 mice with frequent SRS (≥ 3 /h) was randomly chosen for the drug experiments. These 13 mice were used for the vehicle and drug experiments illustrated, so that each mouse received several treatments with washout periods of at least two weeks (mean 2.9 weeks) between two treatments. The order of vehicle and drug administration differed between subgroups of these 13 mice (see Methods). B: In the *Tsc1*^{GFAP} CKO mouse model of TSC, experiments started by EEG electrode implantation at an age of 21–27 days. For each vehicle or drug experiment, a separate group of mice was used (see Methods).

simultaneous digital video-recording of four mice per system using four infrared board cameras (Sony) merged by one video quad processor (Monarcor TVSP-44COL). For video/EEG monitoring, mice were housed singly in clear plexiglass cages. For monitoring during the dark phase, infrared LEDs were mounted above the cages.

As described previously (Riban et al., 2002; Maroso et al., 2011; Twele et al., 2016b), electroclinical and two types of electrographic SRS were recorded in epileptic mice. Focal and secondarily generalized electroclinical seizures were only rarely observed and thus not used as readout for the pharmacological studies. In contrast to the infrequent electroclinical seizures, highly frequent ($\geq 3/h$) focal electrographic seizures occurred in the EEG recorded from the kainate focus in the CA1. Based on their morphology, these electrographic seizures were differentiated into high-voltage sharp waves (HVSWS) and hippocampal paroxysmal discharges (HPDs) as described by us in detail recently (Twele et al., 2016b). Such electrographic seizures are not observed in sham controls (Twele et al., 2017). In short, HVSWS are characterized by sharp waves with high amplitude of at least 3-times the EEG baseline, a frequency of at least 2 Hz, and an inter-event interval of at least 3 s. During the inter-event interval, there is either no epileptic EEG activity or only spikes with low amplitude. HVSWS can either show no clear evolution or some evolution in frequency or pattern. A typical HVSWS is shown in Fig. 3A. HPDs typically start with large amplitude HVSWS, followed by a train of lower-amplitude spikes of at least 5 s of increased frequency ($\geq 5\text{Hz}$; Fig. 3B). Similar to HVSWS, an inter-event interval of at least 3 s is also used for HPDs. During this inter-event interval, there is either no epileptic EEG activity or only spikes with an amplitude of < 2 times the baseline. As shown in Fig. 3B, HPDs exhibit evolution in morphology and frequency, which is not always seen with HVSWS. In addition to these typical HPDs, a second type was observed, which looked like a mixed event starting with HPD-like activity but then evolving into HVSWS-like activity. This type of mixed activity was assigned to HPDs when we counted HVSWSs and HPDs. As described previously (Twele et al., 2016b), the duration of HVSWSs was at least 5 s,

while HPDs were either short (5–20 s) or long (> 20 s). HPDs could only be detected near to the kainate focus in the ipsilateral hippocampus, suggesting focal hippocampal seizures resembling hypersynchronous high voltage spikes observed in sclerotic hippocampus of patients with TLE (Riban et al., 2002). During direct observation of epileptic mice or in the videos recorded during hippocampal HVSWSs and HPDs, no clear behavioral alterations were seen, but subtle alterations may have been overlooked.

To analyze the highly frequent HPDs and HVSWSs, we used a Lab-Chart®-based algorithm, developed for efficient and large-scale EEG analysis of early and late seizures, spikes, and spike clusters in the EEG of a mouse model of viral encephalitis-induced epilepsy (Anjum et al., 2018). This algorithm automatically detects and removes about 80% of high-amplitude EEG artifacts (e.g., due to animal movement, head scratching, grooming, chewing, or drinking), but some low-amplitude artifacts are detected and removed by visual inspection of EEGs and corresponding videos. For the present study, the algorithm was modified to allow automatic detection and differentiation of HPDs and HVSWSs. For this, we used the definition of HPDs and HVSWSs described above except that an amplitude of at least 2 times the EEG baseline (instead of 3 times) was used as criterion, because preliminary data in epileptic CD-1 mice indicated that this results in less variation of seizure frequency when seizures are detected by the algorithm. The data were normalized and threshold values calculated for spike amplitude, Teager energy, and slope by using a median of minimum and maximum values averaged over 200 data points or a 1-sec moving window, as described earlier (Anjum et al., 2018). The algorithm scanned the data for HVSWSs and HPDs, respectively, based on spike frequency and duration of each event as defined previously by our group (Twele et al., 2016b). The algorithm detected the event automatically, but the investigators visualized the electrographic activity simultaneously, therefore assuring the correct identification of the different types of seizures.

Sensitivity and specificity of the algorithm to correctly identify HPDs and HVSWSs in the EEG were assessed by comparing SRS detected during

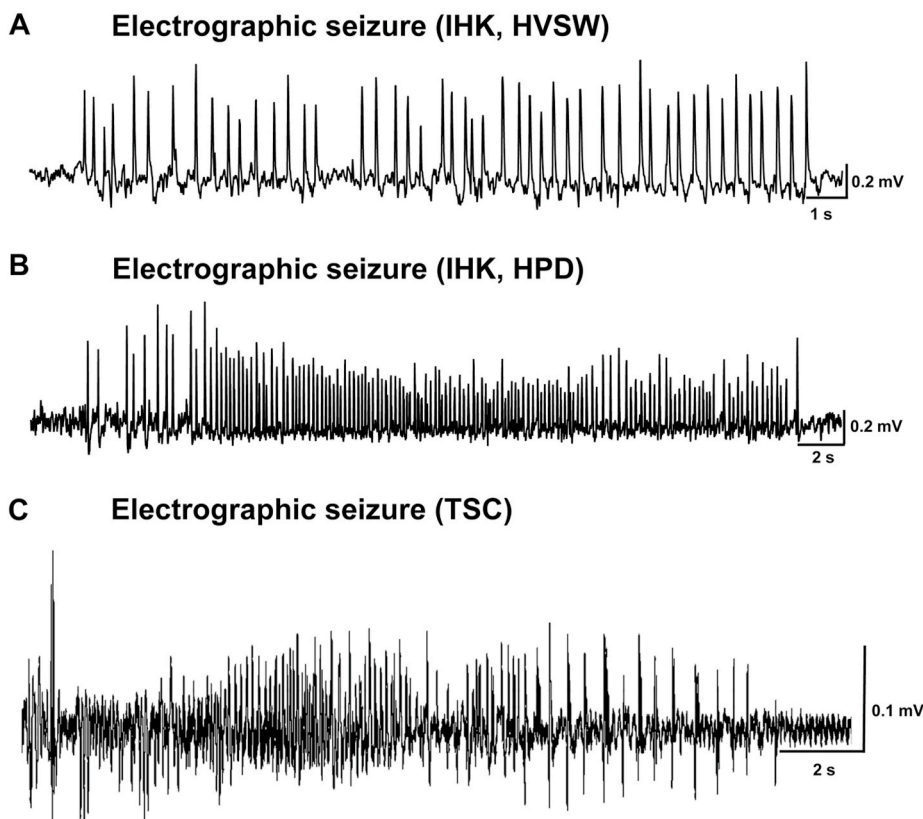


Fig. 3. Representative spontaneous electrographic seizures recorded from the ipsilateral hippocampus in the intrahippocampal kainate mouse model (A, B) or from cortical electrodes in the TSC mouse model (C). Electrographic seizures in epileptic mice of the intrahippocampal kainate model are either monomorphic high-voltage sharp waves (HVSWSs) as illustrated in (A) or polymorphic hippocampal paroxysmal discharge (HPD) as shown in (B). Most HPDs start with HVSWS-like activity, followed by increased spike frequency but lower spike amplitude compared to HVSWSs. (C) Electrographic seizures in *Tsc1^{GFP}*CKO mice are characterized by a stereotypical pattern involving an initial onset of a tonic, repetitive spike discharge followed by a progressive evolution in spike amplitude and frequency that usually culminates in a bursting pattern and postictal suppression.

visual EEG analyses by experienced experimenters with SRS detected by the algorithm in the same EEG samples of nine epileptic mice. For the calculation of these statistical values, an algorithm was run by a person blind to the visually analyzed data and both sets of results were then compared to calculate sensitivity and specificity. These experiments showed that the algorithm was able to detect the different types of SRS that we characterized by visual EEG analysis with a sensitivity of 86–90% and specificity ranging from 90 to 99%.

Operator variability on the algorithm outcome was also assessed. Analyzing the same 24-h EEG twice by different investigators resulted in a correspondence of 100% for HPD events and duration, 98.9% for HVSW event, and 99% for HVSW duration.

Overall, 24/7 EEG data from 13 CD-1 mice were analyzed. Compared to visual EEG inspection, EEG analysis by the algorithm reduced the time needed for analysis by >80% (Anjum et al., 2018). In some experiments, individual data had to be excluded from final analysis because mice did not exhibit SRS on the predrug control day or large parts of the EEG were affected by artifacts (see Figs. 4 and 5 for individual number of mice per experiment).

2.3. Drug studies in intrahippocampal kainate (IHK) mouse model

The treatment protocol used here (see Fig. 2A) was based on a previous study by Huang et al. (2010), in which rapamycin (5 mg/kg i.p. once daily) was administered in epileptic rats for three consecutive days, followed by treatment on every other day for a total of three weeks; a suppressive effect on SRS was observed within the first couple of days. We therefore decided to administer all drugs over 3 consecutive days. Another reason for this prolonged treatment was that preliminary experiments with a single dose treatment, using 5 mg/kg i.p. rapamycin, failed to show any significant effect on SRS frequency (not illustrated).

Using epileptic mice with frequent SRS ($\geq 3/h$), each drug experiment consisted of video-EEG recording for 24 h before drug administration, followed by 3 days with once daily drug administration (Fig. 2A). In each mouse, the video-EEG was continuously recorded over the four days of the experiment. Vehicle controls were treated in the same way. The same groups of mice were used for several experiments with inter-experiment intervals (i.e., drug washout periods) of at least 2 weeks (mean 2.9 weeks, range 2–6.5 weeks), to exclude carry-over effects of the drug treatment. The laborious experiments were performed in two cohorts, using a total of 56 CD-1 mice for the IHK model (36 mice in the first and 20 mice in the second cohort). Of these, a total of 13 CD-1 mice with frequent SRS ($\geq 3/h$) was randomly chosen for the drug experiments. Experiments in these 13 mice were performed in three subgroups of 4–5 mice each. In these subgroups, experiments always started with administration of a drug vehicle (see Fig. 2A), but the subsequent order of administration of the five different drugs (see below) was randomly chosen in each subgroup. For final analysis, data of the three subgroups were combined for each treatment.

All compounds were dissolved in 20% sulfoethyl- β -cyclodextrin (SBECD or Captisol®; Cyclolab, Hungary). For preparation of drug solution, substances were mixed with 20% SBECD solution and sonicated in an ultrasound water bath. 0.02 M HCl was added dropwise until the pH of the solution was 3 ± 0.1 . Vehicle and drug solutions were passed through a 0.2 μ m filter unit and stored at 4 °C. Vehicle and drug solutions were prepared once a week. In preliminary experiments with rapamycin, we used a vehicle consisting of 4% ethanol, 5% polyethylene glycol (PEG) 400 and 5% Tween 80; this vehicle had also been used in previous experiments with rapamycin (Brandt et al., 2018). Therefore, this vehicle was used for comparison with SBECD (Captisol) vehicle in the experiments in the IHK model, to exclude that vehicles *per se* exerted an effect on SRS.

All compounds (and vehicles) were administered orally (p.o.) by gavage in a volume of 10 ml/kg once daily at the following doses: rapamycin, 5 mg/kg; everolimus, 5 mg/kg; PQR530 (as hydrochloride), 25 mg/kg; PQR620 (as hydrochloride), 100 mg/kg; PQR626 (as

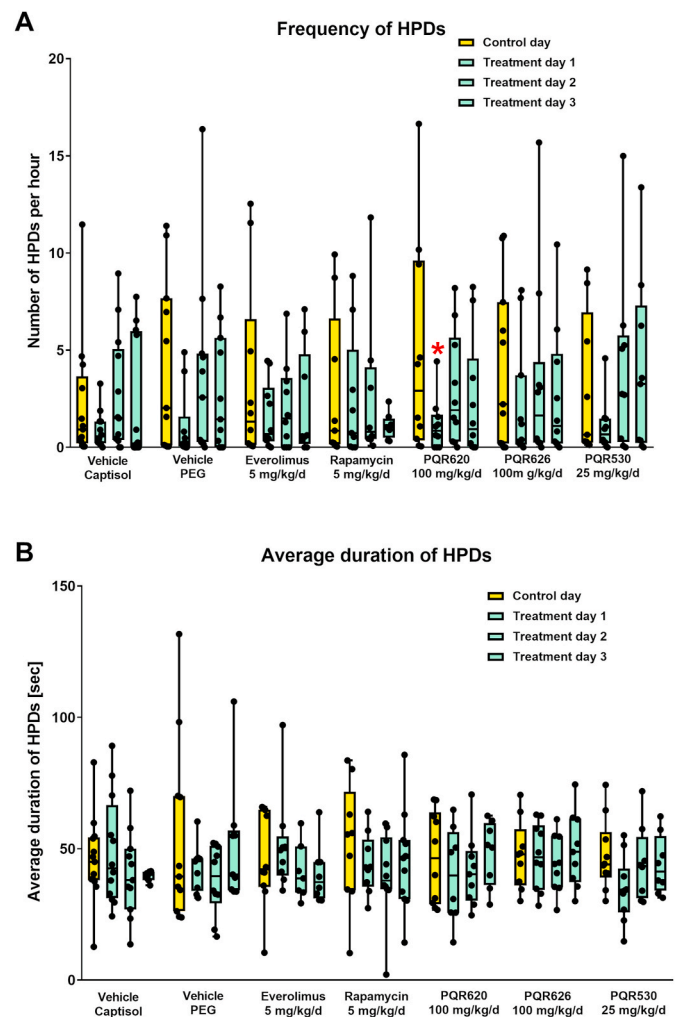


Fig. 4. Effect of prolonged oral treatment with allosteric mTORC1 inhibitors (rapamycin and everolimus), catalytic mTORC1/2 inhibitors (PQR620, PQR626) or a dual pan-PI3K/mTORC1/2 inhibitor (PQR530) on spontaneous hippocampal paroxysmal discharges (HPDs) recorded from the ipsilateral hippocampus in epileptic mice of the intrahippocampal kainate model. A group of 13 epileptic CD-1 mice with frequent electrographic seizures during predrug control experiments was used for the drug trials illustrated in the figure. Each drug or drug vehicle trial consisted of continuous video-EEG recording for 24 h before drug administration (control day), followed by 3 consecutive treatment days with once daily oral drug administration (by gavage) and continuous video-EEG monitoring. The same mice were used for several experiments with inter-experiment intervals of at least two weeks. Two different drug vehicles (captisol and PEG) were compared (see Methods). Data are shown as boxplots with whiskers from minimum to maximal values; the horizontal line in the boxes represents the median value. In addition, individual data are shown. In some experiments, individual data had to be excluded from final analysis because mice did not exhibit SRS on the predrug control day or large parts of the EEG were affected by artifacts; thus, group size of the individual experiments shown here ranged between 7 and 13. Significant differences to the control day of each drug or vehicle trial are indicated by asterisks (* $P = 0.0195$). (A) Frequency of HPDs per hour. (B) Average duration of HPDs in sec.

hydrochloride), 100 mg/kg. These doses have previously been shown to block mTORC1/2 or PI3K/mTORC1/2 in the brain of epileptic mice from the IHK model or naïve mice (Shima et al., 2015; Gericke et al., 2020; Borsari et al., 2020).

2.4. TSC mouse model

We used a previously established mouse model of TSC with

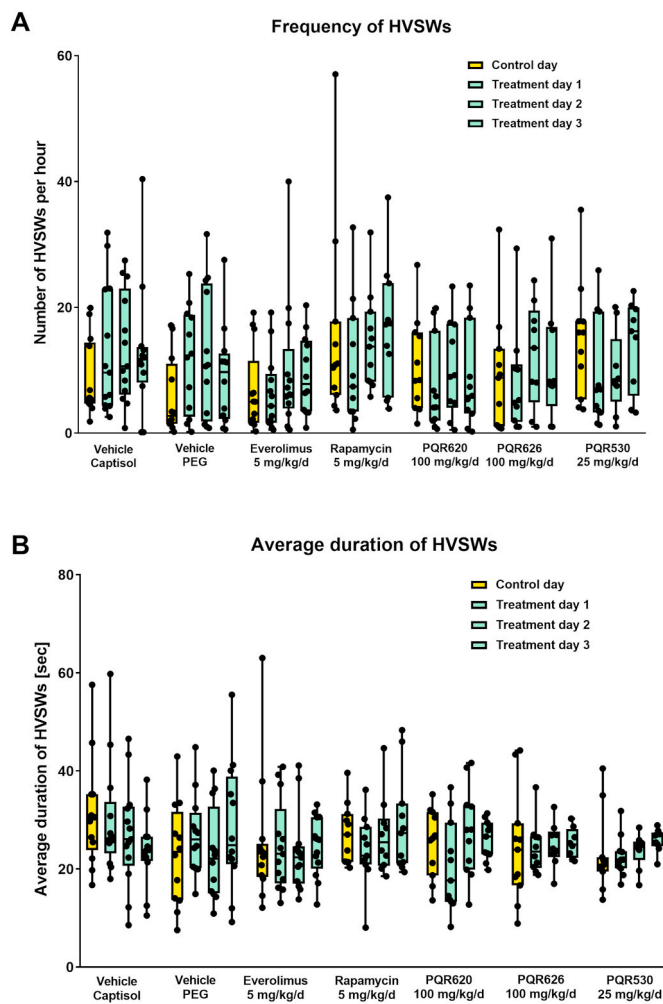


Fig. 5. Effect of prolonged oral treatment with allosteric mTORC1 inhibitors (rapamycin and everolimus), catalytic mTORC1/2 inhibitors (PQR620, PQR626) or a dual pan-PI3K/mTORC1/2 inhibitor (PQR530) on spontaneous high-voltage sharp waves (HVSWs) recorded from the ipsilateral hippocampus in epileptic mice of the intrahippocampal kainate model. A group of 13 epileptic CD-1 mice with frequent electrographic seizures during predrug control experiments was used for the drug trials illustrated in the figure. Each drug or drug vehicle trial consisted of continuous video-EEG recording for 24 h before drug administration (control day), followed by 3 consecutive treatment days with once daily oral drug administration (by gavage) and continuous video-EEG monitoring. The same mice were used for several experiments with inter-experiment intervals of at least two weeks. Two different drug vehicles (captisol and PEG) were compared (see Methods). Data are shown as boxplots with whiskers from minimum to maximal values; the horizontal line in the boxes represents the median value. In addition, individual data are shown. In some experiments, individual data had to be excluded from final analysis because mice did not exhibit SRS on the predrug control day or large parts of the EEG were affected by artifacts; thus, group size of the individual experiments shown here ranged between 7 and 13. No significant differences to the control day were found for any treatment. (A) Frequency of HVSWs per hour. (B) Average duration of HVSWs in sec.

conditional inactivation of the *Tsc1* gene in glial fibrillary acidic protein (GFAP)-positive cells (*Tsc1*^{GFAP} CKO mice), which develops progressive epilepsy beginning at approximately 4 weeks of age, encephalopathy, and premature death with 100 percent penetrance (Uhlmann et al., 2002). *Tsc1*^{GFAP} CKO mice were anesthetized with isoflurane with homeostatic heating to maintain core temperature at 37 ± 1 °C. An 8201-EEG head mount (Pinnacle Technology, Inc., Lawrence, KS) with bihemispheric leads in the frontal and parietal cortices and an indwelling local field potential electrode targeting the region above the

CA1 were used. Before, during, and after surgery, animals were administered fluids, nutrition, antibiotics, and analgesics as required/recommended by the Program of Veterinary Care (PVC) team and IACUC, in concert with the Attending Veterinarian and/or according to IACUC Guidelines of PsychoGenics.

Mice were implanted with electrodes at the age of postnatal day (PND) 21 to PND27 (Fig. 2B). Starting at PND35, EEG was recorded continuously using the Pinnacle Technology 8206 data conditioning and acquisition system (DCAS), and real-time visualization of all EEG channels from all mice was observed using Sirenia or PAL-8400 software. Synchronized video recordings were collected for the duration of the EEG recordings. Electrographic seizures (cf., Zeng et al., 2008) were identified by their characteristic pattern of discrete periods of rhythmic spike discharges that evolved in frequency and amplitude lasting at least 10 s, typically ending with repetitive burst discharges and voltage suppression (see Fig. 3C). Behaviorally, most of the seizures were characterized by a brief period of tonic stiffening of the trunk or extremities without loss of upright posture, followed by a longer period of rhythmic bouncing of the head and trunk with forelimb clonus. Occasionally, other seizures were manifested by a complete behavioral arrest, running movements of the extremities, or severe tonic posturing with loss of upright posture as described previously (Uhlmann et al., 2002).

2.5. Drug studies in TSC mouse model

Vehicle (SBECD) was obtained from DavosPharma (Liberty, MO). The PQR compounds were dissolved in acidified 23.5% SBECD (5.0 ml of 40% SBECD + 3.5 ml of H₂O + 0.2 M HCl as needed). Solution pH was adjusted to be within 2.2 and 2.7 using 0.2 M NaOH and diluted to a final volume of 10.0 ml to yield a vehicle of 20% SBECD (pH 3.0 ± 0.1). Mice in the study were randomly assigned to one of the following treatment groups (Fig. 2B): Vehicle (20% SBECD; PND21-53; p.o. by gavage once a day (q.d.), n = 16), PQR620 (100 mg/kg; PND21-53; p.o. q.d., n = 13), and PQR530 (25 mg/kg; PND21-53; p.o. q.d., n = 14). Dosing was performed during the light cycle phase. Stock 40% SBECD was stored at 4 °C. Vehicle and compound solutions were prepared fresh weekly and administered at 10 ml/kg. Data on PQR620 in the TSC mouse model has been published recently (Rageot et al., 2018) and are included here for comparison with PQR530.

For experiments with rapamycin, mice were randomly assigned to one of the following treatment groups (Fig. 2B): (1) vehicle (5% Tween 80, 5% PEG400, 4% ethanol in saline; PND21-48; s.c., q.d., n = 10); (2) rapamycin (3 mg/kg; PND21-48; s.c., q.d., n = 10); or (3) a combination of vehicle (PND21-34; s.c., q.d.) and rapamycin (3 mg/kg; PND35-48; s.c., q.d.), n = 8. Rapamycin was dissolved in the vehicle consisting of 5% Tween 80, 5% PEG400, 4% ethanol in saline. Vehicle and compound solutions were administered at 10 ml/kg.

2.6. Statistics

In the IHK mouse model, the significance of inter-group differences in seizure frequencies and duration were analyzed by nonparametric analysis of variance (ANOVA) with posthoc Dunn's multiple comparison related to vehicle control. Before analysis, few outliers were detected and removed by Grubb's outlier test, using a significance level (alpha) of 0.001. In the TSC mouse model, the significance of inter-group differences in seizure frequencies and body weight were analyzed by two-way ANOVA test with Dunnett's multiple comparison related to vehicle control. Significant differences in mortality were calculated using the chi-square test.

3. Results

3.1. Drug studies in intrahippocampal kainate (IHK) mouse model

In total, seven experiments with 13 epileptic CD-1 mice were

analyzed as illustrated in Figs. 4 and 5. Each experiment lasted 4 days with continuous video-EEG monitoring, so overall 8736 h of video-EEG (or 364 days of continuous EEG) had to be analyzed for SRS.

Epileptic mice of the IHK model exhibited two types of highly frequent electrographic seizures, HVSWs (Fig. 3A) and HPDs (Fig. 3B). In addition, electroclinical seizures were observed, which were, however, too infrequent to allow analysis of drug effects with the current experimental design. As shown in Fig. 2, the experimental design consisted of one day of pretreatment control, followed by three consecutive treatment days with either vehicle or mTOR inhibitors. Individual frequencies of HPDs and HVSWs largely varied (Figs. 4 and 5). The median frequency of HPDs during the pretreatment control days ranged between 0.2 and 2.9 HPDs per hour (Fig. 4A), whereas median frequency of HVSWs ranged between 2.7 and 16 HVSWs per hour (Fig. 5A). Median duration of HPDs ranged between 40 and 55 s (Fig. 4B), whereas median duration of HVSWs ranged between 21 and 31 s (Fig. 5B).

With one exception, none of the various treatments (including the vehicles) exerted any significant effect on frequency or duration of spontaneous electrographic seizures in the IHK model (Figs. 4 and 5). Only with PQR620 a significant decrease in the frequency of HPDs was observed at the first day of treatment ($p = 0.0195$), but this effect disappeared at subsequent treatment days (Fig. 4A). A similar transient trend was observed with PQR530, but this was not significantly different from pretreatment control ($p = 0.1349$). With rapamycin, mice appeared to exhibit less HPDs on the third day of treatment but, again, this was not significantly different from pretreatment control ($p = 0.2212$).

3.2. Drug studies in TSC mouse model

As previously reported (Uhlmann et al., 2002; Erbayat-Altay et al., 2007), vehicle treated *Tsc1*^{GFAP} CKO mice exhibited frequent spontaneous electrographic seizures. A representative EEG trace is shown in Fig. 3C, while the frequency of these SRS is shown in Fig. 6. Prolonged daily treatment with either PQR530 or PQR620 almost completely suppressed the seizures (Fig. 6A). This significant antiseizure effect ($p < 0.05$) was not transient but remained at about the same level over the treatment period.

Mice with conditional inactivation of the *Tsc1* gene primarily in glia (*Tsc1*^{GFAP} CKO mice) develop glial proliferation, progressive epilepsy, and premature death (Uhlmann et al., 2002; Erbayat-Altay et al., 2007; Zeng et al., 2008). Survival curves may differ across different cohorts of *Tsc1*^{GFAP} CKO mice. For instance, Zeng et al. (2008) reported that 50% of vehicle-treated *Tsc1*^{GFAP} CKO mice died by 9 weeks of age, with no survival by 4 months, while Uhlmann et al. (2002) observed that mice began to die at 3–4 months. In the present experiments, 30% of the vehicle-treated mice died by 8 weeks of age, which was not significantly altered by treatment with PQR530 or PQR620 before animals were sacrificed at the end of the study (at PND55).

For rapamycin, two different treatment regimens were compared (Figs. 2 and 6B). Mice treated with 3 mg/kg rapamycin from PND21–48 exhibited no seizures. Thus, the efficacy of this treatment regimen of rapamycin was comparable to the efficacies observed with PQR530 and PQR620. A second group that received vehicle from PND21–35 and rapamycin (3 mg/kg) from PND36–48 showed no significant reduction in the number of seizures at week 6 but a significant reduction at week 7 ($p < 0.05$).

Nine out of 26 mice (~35%) that received vehicle treatment beginning PND21 perished by PND34 while no mortality was observed in the rapamycin treated group ($P = 0.032$). Survival rate was also examined across groups from the start of PND35 to PND48. By the end of week 7, the vehicle only group sustained a mortality of 40% whereas 0% mortality was recorded in the rapamycin-treated groups ($P = 0.015$).

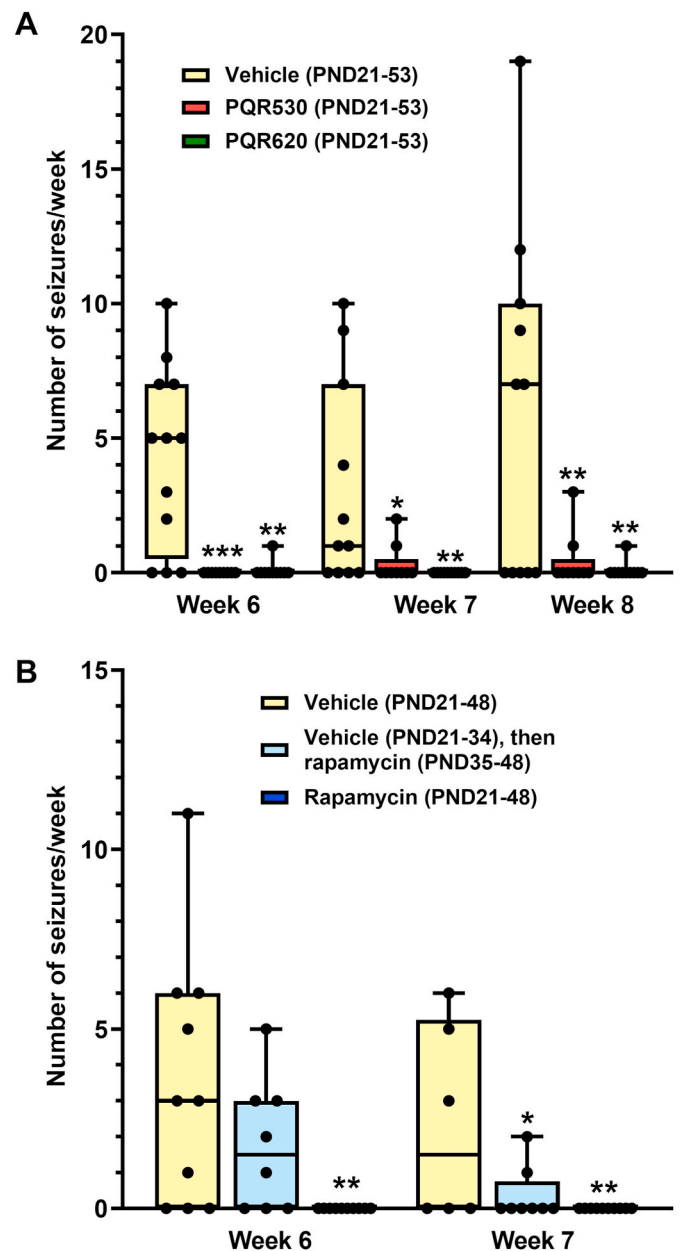


Fig. 6. Effects of mTOR and PI3K inhibitors on frequency of spontaneous electrographic seizures caused by elimination of *Tsc1* in GFAP-expressing cells. Data are shown as boxplots with whiskers from minimum to maximal values; the horizontal line in the boxes represents the median value. In addition, individual data are shown. Significant differences to the vehicle only group are indicated by asterisk (* $P < 0.05$; ** $P < 0.01$; *** $P < 0.0001$). (A) *Tsc1*^{GFAP} conditional knockout (CKO) mice were treated postnatal days (PND) 21–53 with vehicle, PQR530 (25 mg/kg once per day by oral gavage), or PQR620 (100 mg/kg/day p.o.) and EEG was monitored continuously during PND35–53. (B) Effect of rapamycin on spontaneous electrographic seizures in *Tsc1*^{GFAP} CKO mice. One group of mice received vehicle during PND21–48; a second group received vehicle during PND21–34 and then rapamycin (3 mg/kg once daily s.c.) during PND35–48; a third group received rapamycin (3 mg/kg once daily s.c.) during PND21–48. Numbers of mice in vehicle groups decrease over time due to death of some animals, as expected.

3.3. Tolerability

In the present study, no quantitative evaluation of adverse events was performed during the experiments, but mice were closely observed for any obvious behavioral alterations. As described previously (Brandt

et al., 2018), the only observable adverse effect of treatments with mTOR inhibitors was moderate sedation. When body weight was monitored during the treatment period in *Tsc1^{GFAP}* CKO mice, both PQR530 and PQR620 caused a moderate (~20%) and transient decrease in body weight gain of female mice in the first two weeks of treatment, but this disappeared during the remaining treatment period (Fig. 7A). A similar transient effect on body weight gain was observed in male mice (Fig. 7B). Rapamycin did not decrease body weight gain (Fig. 7C and D).

4. Discussion

The PI3K/Akt/mTOR pathway, which is a central player of intracellular signaling in the brain by regulating neuronal survival, growth, and plasticity, becomes hyperactive following epileptogenic brain injury in animal models and in humans with acquired forms of epilepsy (Gal-anopoulou et al., 2012; Wong, 2013; Citraro et al., 2016). To our knowledge, only two previous studies examined the efficacy of mTOR

inhibitors to block SRS in rodent models of acquired epilepsy. In the study of Huang et al. (2010), rats with SRS developing after pilocarpine-induced SE were treated for three weeks with rapamycin 5 mg/kg or vehicle daily for the first three days and then every other day for the remaining treatment period. Rapamycin treatment markedly reduced seizure frequency recorded over the 3 weeks of treatment. To determine when this inhibitory effect of rapamycin treatment on chronic SRS began, Huang et al. (2010) quantified seizure activity over a five-day period beginning 24 h after the first rapamycin injection and observed that the significant reduction in seizure frequency began shortly after onset of treatment. However, the antiseizure effect of rapamycin seemed to be restricted to generalized convulsive SRS, whereas focal non-convulsive seizures were not suppressed. Furthermore, SRS were only recorded by video for 12 h/day, so focal electrographic seizures were not monitored. This may partially explain why Buckmaster and Lew (2011), who used continuous (24/7) video/EEG monitoring of SRS in the pilocarpine model of TLE in mice, did not

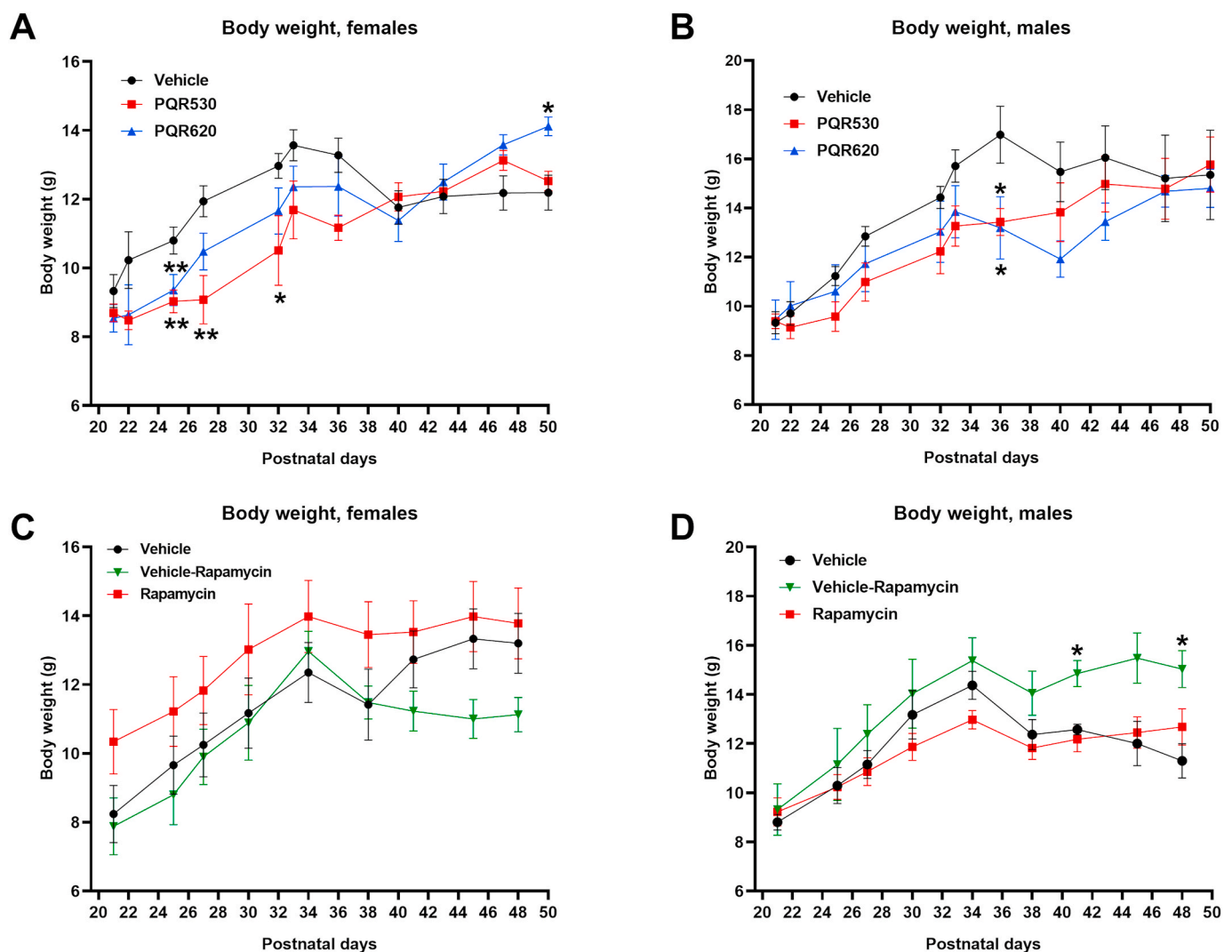


Fig. 7. Effects of mTOR and PI3K inhibitors on body weight in *Tsc1^{GFAP}* conditional knockout (CKO) mice. Mice are the same in which seizures were recorded as shown in Fig. 6. Data are shown as means \pm SEM; the body weight on postnatal day (PND) 21 was measured before onset of treatment. Significant differences to body weight in vehicle controls are indicated by asterisk (* $P < 0.05$; ** $P < 0.01$). A: Female *Tsc1^{GFAP}* CKO mice were treated on postnatal days (PND) 21–53 with vehicle ($n = 8$), PQR530 (25 mg/kg once per day by oral gavage; $n = 6$), or PQR620 (100 mg/kg/day p.o.; $n = 6$). B: Male *Tsc1^{GFAP}* CKO mice were treated on PND21–53 with vehicle ($n = 8$), PQR530 (25 mg/kg once per day by oral gavage; $n = 8$), or PQR620 (100 mg/kg/day p.o.; $n = 7$). C: Female *Tsc1^{GFAP}* CKO mice ($n = 7$) were treated with vehicle during PND21–48; a second group (“vehicle– rapamycin”; $n = 4$) received vehicle during PND21–34 and then rapamycin (3 mg/kg once daily s. c.) during PND35–48; a third group ($n = 4$) received rapamycin (3 mg/kg once daily s.c.) during PND21–48. D: Male *Tsc1^{GFAP}* CKO mice ($n = 3$) were treated with vehicle during PND21–48; a second group (“vehicle– rapamycin”; $n = 4$) received vehicle during PND21–34 and then rapamycin (3 mg/kg once daily s.c.) during PND35–48; a third group ($n = 6$) received rapamycin (3 mg/kg once daily s.c.) during PND21–48.

observe any significant antiseizure effect during chronic treatment with rapamycin, although the treatment suppressed mossy fiber sprouting.

We recently determined the electrical seizure threshold in epileptic mice of the pilocarpine model and found that everolimus (5 mg/kg p.o.) was much more effective than rapamycin (5 mg/kg i.p. or p.o.) to increase seizure threshold (Brandt et al., 2018). Furthermore, the novel catalytic mTORC1/C2 inhibitor PQR620 was more effective than rapamycin and the catalytic dual pan-PI3K/mTORC1/2 inhibitor PQR530 to increase seizure threshold in epileptic mice (Brandt et al., 2018). Interestingly, everolimus was also significantly more effective than rapamycin to attenuate neuroinflammation in response to kainate in mice (Yang et al., 2017). Neuroinflammation in response to kainate treatment was not mediated through the Akt pathway but was primarily mediated by phosphorylation of extracellular signal related kinase (ERK), which was more effectively attenuated by everolimus than by rapamycin (Yang et al., 2017). Everolimus is significantly more effective in inhibiting mTORC2 activation than rapamycin (Jin et al., 2014) and so is PQR620 (Brandt et al., 2018; Rageot et al., 2018). It is generally believed that many of the neurologic consequences of mTOR pathway dysfunction are due to dysregulation of mTORC1 activity rather than of mTORC2 (Crino, 2016). However, this dogma has been challenged recently (Chen et al., 2019; Jansen, 2020), which will be discussed below.

In the present study, neither the allosteric mTORC1 inhibitors rapamycin and everolimus nor the novel catalytic mTORC1/2 or dual pan-PI3K/mTORC1/2 inhibitors were capable of significantly suppressing spontaneous electrographic seizures in the IHK model of acquired TLE. The only exception was a transient antiseizure effect of PQR620 on HPDs. These data thus substantiate and extend the findings of Buckmaster and Lew (2011) in the pilocarpine model of TLE in mice and indicate that SRS in such models are resistant to mTOR or PI3K/mTOR inhibitors when analyses are based on continuous video-EEG monitoring.

In contrast to the negative outcome of the IHK experiments, in the *Tsc1*^{GFP} CKO mouse model, both PQR530 and PQR620 were highly efficacious suppressing SRS when administered once daily over 3 weeks. Similarly, as reported previously (Zeng et al., 2008), the allosteric mTOR inhibitor rapamycin suppressed SRS. In a study by Meikle et al. (Meikle et al., 2008) in a neuronal mouse model of TSC in which *Tsc1* is ablated in most neurons during cortical development, it was mentioned that mice treated with everolimus (6 mg/kg i.p. every other day) did not exhibit spontaneous clinical seizures, but data from seizure monitoring were not shown.

With respect to survival of *Tsc1*^{GFP} CKO mice, no significant effects of PQR530 or PQR620 were observed in the present study, in which animals were treated from PND21-53. In contrast, when mice were treated with PQR620 (100 mg/kg p.o. once daily) or PQR626 (50 mg/kg p.o., twice daily) from PND21 to PND90, both compounds significantly prevented or decreased mortality as compared to vehicle controls (Borsari et al., 2020), which is similar to the effects reported previously for rapamycin (Zeng et al., 2008) and everolimus (Meikle et al., 2008).

In contrast to PQR530, PQR620 and PQR626, rapamycin primarily inhibits mTORC1, although chronic exposure to rapamycin has been demonstrated to also inhibit mTORC2 activity, potentially through a reduction of mTOR availability for formation of the complex (Saxton and Sabatini, 2017). mTORC1 and mTORC2 are structurally and functionally distinct complexes. mTORC1 is comprised of a group of binding proteins including the regulatory-associated protein of mTOR (raptor) and controls cell growth, cell proliferation, cell survival, and cell death via modulating protein synthesis and autophagy (Laplante and Sabatini, 2012; Switon et al., 2017). Overactivation of mTORC1 has been observed in numerous brain pathologies, including TSC, characterized by neocortical gliosis, migratory heterotopia, neuron mispositioning, and cell hypertrophy (Jeong and Wong, 2015). In contrast to mTORC1, mTORC2 complexes with a separate group of accessory proteins including rapamycin-insensitive companion of mTOR (riCTOR), and

modulates processes related to cell structure and metabolism (Laplante and Sabatini, 2012; Switon et al., 2017). In the brain, mTORC2 has an important role in cell survival and in the maintenance of the actin cytoskeleton and is implicated in the morphological regulation of actin-rich dendritic spines (Lipton and Sahin, 2014). Furthermore, mTORC2 controls several neuroprotective signaling pathways through phosphorylation of Akt at Ser473 (Laplante and Sabatini, 2012; Switon et al., 2017).

Both, mTORC1 and mTORC2, are activated in human TLE (Talos et al., 2018) and chronic rodent models of TLE (Goto et al., 2010; Lopes et al., 2012; Brewster et al., 2013). Talos et al. (2018) suggested that the strong neuroprotective mechanisms triggered by mTORC2 activation is an argument against using total mTOR blockade by second-generation inhibitors targeting the mTOR catalytic site (dual mTORC1 and mTORC2 inhibitors). This suggestion, however, is mainly based on theoretical considerations. Indeed, in contrast to this suggestion, the dual mTORC1 and mTORC2 inhibitor, KU0063794, is neuroprotective after spinal cord injury in mice (Cordaro et al., 2017), and knockdown of rictor, a key component of mTORC2, has been shown to enhance neuroprotective activity of rapamycin in primary neurons (Xu et al., 2015). The present data in *Tsc1*^{GFP} CKO mice with the catalytic inhibitors PQR530 and PQR620, which inhibit both mTORC1 and mTORC2, strongly suggest that concomitant inhibition of mTORC2 does not impair the antiseizure effect compared to selective mTORC1 inhibitors such as rapamycin. Furthermore, in a recent study in a mouse model of a mTORopathy resulting from loss-of-function mutations in the phosphatase and tensin homolog (*PTEN*) gene, genetic deletion of mTORC2 (but not mTORC1) activity prolonged lifespan, suppressed seizures, and normalized metabolic changes in the brain of mice lacking *Pten* (Chen et al., 2019). It is important to learn more about the role of mTORC2 in epilepsy or epileptogenesis in other mTORopathies, including TSC.

In addition to inhibiting both mTORC1 and mTORC2, the small molecule 1,3,5-triazine derivatives PQR530, PQR620 and PQR626 rapidly penetrate into the brain, reach brain:plasma levels of >1, and are eliminated from mouse brain with a half-life of only ~2–5 h (Brandt et al., 2018; Rageot et al., 2018, 2019; Borsari et al., 2020). For comparison, rapamycin and everolimus only poorly penetrate into the brain (brain:plasma ratios in mice are only 0.0057 and 0.016, respectively), but are very slowly eliminated from the brain (Meikle et al., 2008; Abs et al., 2013; Brandt et al., 2018; Borsari et al., 2020). Thus, high systemic doses of rapalogs are needed to inhibit mTOR in the brain, which may provide an advantage of brain-penetrant novel catalytic mTORC1/C2 inhibitors PQR530 and PQR620 to minimize systemic side effects (Brandt et al., 2018; Borsari et al., 2020). Thus, as indicated by pre-clinical experiments on maximal tolerated doses (MTDs) of the triazine derivatives PQR530, PQR620 and PQR626 in rodents and preclinical and clinical experience with the triazine derivative PQR309 (bimiralisib), the tolerability of the novel ATP-competitive inhibitors is expected to be high with a much broader therapeutic window than observed for rapalogs (Beaufils et al., 2017; Bohnacker et al., 2017; Brandt et al., 2018; Wicki et al., 2018; Hillmann and Fabbro, 2019; Borsari et al., 2020).

The favorable brain penetration of the novel mTOR inhibitors that we reported recently was determined in normal (healthy) mice and rats (Brandt et al., 2018; Rageot et al., 2018, 2019; Borsari et al., 2020). Epilepsy is known to induce alterations in the blood-brain barrier (BBB) in both rodent models and patients, leading for instance to extravasation of albumin and invasion of immune cells from blood into brain parenchyma (van Vliet et al., 2015; Löscher and Friedman, 2020). However, we and others have previously demonstrated in rodent models of TLE that these BBB changes do not lead to increased drug penetration into the brain (Löscher and Friedman, 2020). Instead, drug penetration through the BBB may be restricted by increased expression of efflux transporters such as P-glycoprotein at the BBB (Löscher et al., 2020), but the PQR compounds tested here are not substrates of such transporters (Brandt et al., 2018; Borsari et al., 2020). Thus, it is unlikely that BBB

changes explain that the novel brain-permeant mTOR inhibitors were not more effective than rapalogs in suppressing SRS in the present experiments.

However, in this respect it is important to note that rapamycin is essentially 100% effective in the TSC mouse model at the dose (3 mg/kg/d s.c.) used here, so superiority of the novel PQR compounds is impossible to demonstrate in this situation. Currently, only everolimus is approved for the treatment of partial epilepsy with SRS in individuals with TSC. The EXIST-3 trial demonstrated efficacy of everolimus on focal seizures in TSC (French et al., 2016; Franz et al., 2018), but the efficacy is far from maximal – many patients did not respond and many more did not respond completely, and the treatment was associated with adverse effects. So there is a need for more efficacious and/or tolerable treatments.

In the present study, slightly different methodology was used for drug testing in the two epilepsy models, because the experiments were performed in two different laboratories that used their standard protocols for pharmacological studies in these models. Differences included the route of administration of rapamycin (p.o. in the IHK model vs. s.c. in the TSC model), the dose of rapamycin (5 mg/kg in the IHK model vs. 3 mg/kg in the TSC model), and the duration of treatment of compounds (3 consecutive days in the IHK model vs. 28–32 days in the TSC model), respectively. The higher dose chosen for oral vs. s.c. administration of rapamycin was based on previous data showing that plasma levels obtained in mice were lower with oral than with s.c. administration (Baker et al., 1978). Doses and route of administration of PQR530 and PQR620 were the same in both animal models, but, again, duration of treatment differed between the models. We cannot exclude that these factors made a difference in the seizure response in the IHK vs. TSC mouse models. However, we consider this unlikely because the present data on lack of any antiseizure activity of rapamycin, everolimus or the novel PQR compounds on SRS in the IHK model of TLE are in line with the data reported by Buckmaster and Lew (2011), who found that chronic administration of rapamycin (1.5 or 3 mg/kg once daily i.p. over 2 months, starting 24 h after SE) exerted no antiseizure effects on SRS in the pilocarpine model of TLE in mice. This also suggests that the timing of treatment (≥ 8 weeks after kainate in the present experiments vs. 24 h after pilocarpine in the study of Buckmaster and Lew (2011)) does not play a significant role for the effect of mTOR inhibition on SRS in mouse models of acquired epilepsy. This suggestion is substantiated by our recent study in the IHK model, in which prolonged treatment with PQR530 or PQR620, starting 6 h after kainate, did not prevent the development of SRS (Gericke et al., 2020). In this latter study we also showed that doses and route of administration of the PQR compounds used here block mTORC1/2 or PI3K/mTORC1/2 in the brain of epileptic mice from the IHK model (Gericke et al., 2020).

In conclusion, the present study is the first that compared the antiseizure efficacy of the three current classes of mTOR inhibitors, i.e., allosteric mTORC1 inhibitors (rapamycin, everolimus); dual PI3K/mTOR inhibitors that target both PI3K and mTORC1/mTORC2 (PQR530; Rageot et al., 2019); and ATP-competitive, ‘active-site’ mTORC1/mTORC2 inhibitors, which target the catalytic site of mTOR only (PQR620; Rageot et al., 2018; PQR626; Borsari et al., 2020). The novel ATP-competitive inhibitors differ from other recently developed catalytic mTOR inhibitors (e.g., AZD2014) and the rapalogs rapamycin and everolimus by having much better brain penetration (Brandt et al., 2018; Rageot et al., 2018, 2019; Hillmann and Fabbro, 2019; Borsari et al., 2020), thus favoring their use in neurological disorders such as epilepsy, for which a role of dysregulated PI3K/Akt/mTOR signaling has been suggested. No clear differences in antiseizure efficacy were found across these three classes of mTOR inhibitors in mouse models of genetic and acquired epilepsies. However, the compounds were used at doses which appeared to be maximally effective in the TSC model, and thus dose-response studies may be needed to identify differentiating features in future studies. None of the compounds exerted any robust efficacy in the IHK model of acquired TLE, whereas consistent antiseizure efficacy

was observed in the TSC mouse model. Thus, as indicated by preclinical and clinical data, the main advantage of the novel 1,3,5-triazine derivatives is their potential for improved tolerability compared to rapalogs (Hillmann and Fabbro, 2019), which would favor their development as new therapies for TORopathies such as TSC. Overall, the novel 1,3,5-triazine derivatives have potential, and a different pharmacological profile than rapalogs (Hillmann and Fabbro, 2019), but their superiority over rapalogs in the treatment of neurological disorders such as TSC remains to be shown.

Credit Author Statement

Wiebke Theilmann: Methodology, Investigation, Formal analysis, Validation, Writing - review & editing. **Birthe Gericke:** Formal analysis, Validation, Writing - review & editing. **Alina Schidlitzki:** Supervision, Writing - review & editing. **Syed Muhammad Muneeb Anjum:** Software, Data curation, Writing - review & editing. **Saskia Borsdorf:** Formal analysis, Validation, Writing - review & editing. **Timon Harries:** Formal analysis, Validation, Writing - review & editing. **Steven L. Roberds:** Methodology, Supervision, Writing - review & editing. **Dean J. Aguiar:** Formal analysis, Validation, Writing - review & editing. **Daniela Brunner:** Formal analysis, Validation, Writing - review & editing. **Steven C. Leiser:** Investigation, Methodology, Formal analysis, Writing - review & editing. **Dekun Song:** Formal analysis, Validation, Writing - review & editing. **Doriano Fabbro:** Conceptualization, Resources, Writing - review & editing. **Petra Hillmann:** Conceptualization, Resources, Writing - review & editing. **Matthias P. Wymann:** Conceptualization, Resources, Writing - review & editing. **Wolfgang Löscher:** Conceptualization, Project administration, Methodology, Writing - original draft, preparation, Writing - review & editing.

Acknowledgements

We are thankful to Dr. Michael Wong at Washington University (St. Louis, MO, USA) for licensing and providing advice establishing the *Tsc1*^{GFP}CKO model to the Tuberous Sclerosis Alliance TSC Preclinical Consortium and its partner PsychoGenics. The study was supported by a grant from the Epilepsy Foundation (Landover, MD, USA), the Innosuisse grant 37213.1 IP-LS, the Novartis Foundation for medical-biological Research grant 14B095; and the Swiss National Science Foundation grant 310030_189065 to MPW. We thank Edith Kaczmarek for skillful technical assistance.

References

- Abs, E., Goorden, S.M., Schreiber, J., Overwater, I.E., Hoogveen-Westerveld, M., Bruinsma, C.F., Aganovic, E., Borgesius, N.Z., Nellist, M., Elgersma, Y., 2013. TORC1-dependent epilepsy caused by acute biallelic *Tsc1* deletion in adult mice. *Ann. Neurol.* 74, 569–579.
- Anjum, S.M.M., Käufer, C., Hopfengärtner, R., Waldt, I., Bröer, S., Löscher, W., 2018. Automated quantification of EEG spikes and spike clusters as a new read out in Theiler’s virus mouse model of encephalitis-induced epilepsy. *Epilepsy Behav.* 88, 189–204.
- Baker, H., Sidorowicz, A., Sehgal, S.N., Váczina, C., 1978. Rapamycin (AY-22,989), a new antifungal antibiotic. III. In vitro and in vivo evaluation. *J. Antibiot. (Tokyo)* 31, 539–545.
- Beaufils, F., Cmijanjovic, V., Bohnacker, T., Melone, A., Marone, R., Jackson, E., Zhang, X., Sele, A., Borsari, C., Mestan, J., Hebeisen, P., Hillmann, P., Giese, B., Zvelebil, M., Fabbro, D., Williams, R.L., Rageot, D., Wymann, M.P., 2017. 5-(4,6-Dimorpholino-1,3,5-triazin-2-yl)-4-(trifluoromethyl)pyridin-2-amine (PQR309), a potent, brain-penetrant, orally bioavailable, pan-class I PI3K/mTOR inhibitor as clinical candidate in oncology. *J. Med. Chem.* 60, 7254–7538.
- Bohnacker, T., Protá, A.E., Beaufils, F., Burke, J.E., Melone, A., Inglis, A.J., Rageot, D., Sele, A.M., Cmijanjovic, V., Cmijanjovic, N., Bargsten, K., Aher, A., Akhmanova, A., Diaz, J.F., Fabbro, D., Zvelebil, M., Williams, R.L., Steinmetz, M.O., Wymann, M.P., 2017. Deconvolution of Buparlisib’s mechanism of action defines specific PI3K and tubulin inhibitors for therapeutic intervention. *Nat. Commun.* 8, 14683.
- Borsari, C., Keles, E., Rageot, D., De Pascale, M., Treyer, A., Bohnacker, T., Melone, A., Sriramaratnam, R., Beaufils, F., Hamburger, M., Hebeisen, P., Löscher, W., Fabbro, D., Hillmann, P., Wymann, M.P., 2020. 4-(Difluoromethyl)-5-(4-((3R,5S)-3,5-dimethylmorpholino)-6-((R)-3-methylmorpholino)-1,3,5-triazin-2-yl)pyridin-2-

- amine (PQR626), a potent, orally available, and brain-penetrant mTOR inhibitor for the treatment of neurological disorders. *J. Med. Chem.* *submitted*.
- Bouillieret, V., Ridoux, V., Depaulis, A., Marescaux, C., Nehlig, A., Le Gal, L.S., 1999. Recurrent seizures and hippocampal sclerosis following intrahippocampal kainate injection in adult mice: electroencephalography, histopathology and synaptic reorganization similar to mesial temporal lobe epilepsy. *Neuroscience* 89, 717–729.
- Brandt, C., Hillmann, P., Noack, A., Römermann, K., Öhler, L.A., Rageot, D., Beaufils, F., Melone, A., Sele, A.M., Wymann, M.P., Fabbro, D., Löscher, W., 2018. The novel, catalytic mTORC1/2 inhibitor PQR620 and the PI3K/mTORC1/2 inhibitor PQR530 effectively cross the blood-brain barrier and increase seizure threshold in a mouse model of chronic epilepsy. *Neuropharmacology* 140, 107–120.
- Brewster, A.L., Lugo, J.N., Patil, V.V., Lee, W.L., Qian, Y., Vanegas, F., Anderson, A.E., 2013. Rapamycin reverses status epilepticus-induced memory deficits and dendritic damage. *PLoS One* 8, e57808.
- Buckmaster, P.S., Lew, F.H., 2011. Rapamycin suppresses mossy fiber sprouting but not seizure frequency in a mouse model of temporal lobe epilepsy. *J. Neurosci.* 31, 2337–2347.
- Chen, C.J., Sgritta, M., Mays, J., Zhou, H., Lucero, R., Park, J., Wang, I.C., Park, J.H., Kaiparettu, B.A., Stoica, L., Jafar-Nejad, P., Rigo, F., Chin, J., Noebels, J.L., Costa-Mattoli, M., 2019. Therapeutic inhibition of mTORC2 rescues the behavioral and neurophysiological abnormalities associated with Pten-deficiency. *Nat. Med.* 25, 1684–1690.
- Chia, R., Achilli, F., Festing, M.F., Fisher, E.M., 2005. The origins and uses of mouse outbred stocks. *Nat. Genet.* 37, 1181–1186.
- Chiarini, F., Evangelisti, C., McCubrey, J.A., Martelli, A.M., 2015. Current treatment strategies for inhibiting mTOR in cancer. *Trends Pharmacol. Sci.* 36, 124–135.
- Citraro, R., Leo, A., Constanti, A., Russo, E., De Sarro, G., 2016. mTOR pathway inhibition as a new therapeutic strategy in epilepsy and epileptogenesis. *Pharmacol. Res.* 107, 333–343.
- Cordaro, M., Paterniti, I., Siracusa, R., Impellizzeri, D., Esposito, E., Cuzzocrea, S., 2017. KU063794, a dual mTORC1 and mTORC2 inhibitor, reduces neural tissue damage and locomotor impairment after spinal cord injury in mice. *Mol. Neurobiol.* 54, 2415–2427.
- Crino, P.B., 2016. The mTOR signalling cascade: paving new roads to cure neurological disease. *Nat. Rev. Neurol.* 12, 379–392.
- Devinsky, O., Vezzani, A., O'Brien, T.J., Jette, N., Scheffer, I.E., De Curtis, M., Perucca, P., 2018. Epilepsy. *Nat. Rev. Dis. Primers.* 4, 18024.
- Duveau, V., Roucard, C., 2017. A mesiotemporal lobe epilepsy mouse model. *Neurochem. Res.* 42, 1919–1925.
- Erbayat-Altay, E., Zeng, L.H., Xu, L., Gutmann, D.H., Wong, M., 2007. The natural history and treatment of epilepsy in a murine model of tuberous sclerosis. *Epilepsia* 48, 1470–1476.
- Franz, D.N., Belousova, E., Sparagana, S., Bebin, E.M., Frost, M.D., Kuperman, R., Witt, O., Kohrman, M.H., Flamini, J.R., Wu, J.Y., Curatolo, P., de Vries, P.J., Berkowitz, N., Niolat, J., Jozwiak, S., 2016. Long-term use of everolimus in patients with tuberous sclerosis complex: final results from the EXIST-1 study. *PLoS One* 11, e0158476.
- Franz, D.N., Lawson, J.A., Yapici, Z., Ikeda, H., Polster, T., Nabbutt, R., Curatolo, P., de Vries, P.J., Dlugos, D.J., Voi, M., Fan, J., Vauury, A., Pelov, D., French, J.A., 2018. Everolimus for treatment-refractory seizures in TSC: extension of a randomized controlled trial. *Neurol. Clin. Pract.* 8, 412–420.
- French, J.A., Lawson, J.A., Yapici, Z., Ikeda, H., Polster, T., Nabbutt, R., Curatolo, P., de Vries, P.J., Dlugos, D.J., Berkowitz, N., Voi, M., Peyrard, S., Pelov, D., Franz, D.N., 2016. Adjunctive everolimus therapy for treatment-resistant focal-onset seizures associated with tuberous sclerosis (EXIST-3): a phase 3, randomised, double-blind, placebo-controlled study. *Lancet* 388, 2153–2163.
- Galanopoulou, A.S., Gorter, J.A., Cepeda, C., 2012. Finding a better drug for epilepsy: the mTOR pathway as an antiepileptogenic target. *Epilepsia* 53, 1119–1130.
- Gericke, B., Brandt, C., Theilmann, W., Welzel, L., Schidlitzki, A., Twele, F., Kaczmarek, E., Anjum, M., Hillmann, P., Löscher, W., 2020. Selective inhibition of mTORC1/2 or PI3K/mTORC1/2 signaling does not prevent or modify epilepsy in the intrahippocampal kainate mouse model. *Neuropharmacology* 162, 107817.
- Godale, C.M., Danzer, S.C., 2018. Signaling pathways and cellular mechanisms regulating mossy fiber sprouting in the development of epilepsy. *Front. Neurol.* 9, 298.
- Goto, E.M., Silva, M.P., Perosa, S.R., Arganaraz, G.A., Pesquero, J.B., Cavalheiro, E.A., Naffah-Mazzacoratti, M.G., Teixeira, V.P., Silva Jr., J.A., 2010. Akt pathway activation and increased neuropeptide Y mRNA expression in the rat hippocampus: implications for seizure blockade. *Neuropeptides* 44, 169–176.
- Griffith, J.L., Wong, M., 2018. The mTOR pathway in treatment of epilepsy: a clinical update. *Future Neurol.* 13, 49–58.
- Hassan, B., Akcakanat, A., Sangai, T., Evans, K.W., Adkins, F., Eterovic, A.K., Zhao, H., Chen, K., Chen, H., Do, K.A., Xie, S.M., Holder, A.M., Naing, A., Mills, G.B., Meric-Bernstam, F., 2014. Catalytic mTOR inhibitors can overcome intrinsic and acquired resistance to allosteric mTOR inhibitors. *Oncotarget* 5, 8544–8557.
- Henshall, D.C., 2017. Poststatus epilepticus models: focal kainic acid. In: Pitkänen, A., Buckmaster, P.S., Galanopoulou, A.S., Moshé, S.L. (Eds.), *Models of Seizures and Epilepsy*, second ed. Academic Press, London, pp. 611–624.
- Hillmann, P., Fabbro, D., 2019. PI3K/mTOR pathway inhibition: opportunities in oncology and rare genetic diseases. *Int. J. Mol. Sci.* 20.
- Huang, X., Zhang, H., Yang, J., Wu, J., McMahon, J., Lin, Y., Cao, Z., Gruenthal, M., Huang, Y., 2010. Pharmacological inhibition of the mammalian target of rapamycin pathway suppresses acquired epilepsy. *Neurobiol. Dis.* 40, 193–199.
- Janku, F., Yap, T.A., Meric-Bernstam, F., 2018. Targeting the PI3K pathway in cancer: are we making headway? *Nat. Rev. Clin. Oncol.* 15, 273–291.
- Jansen, L.A., 2020. mTORC2 steals the spotlight. *Epilepsy Current* 20, 116–117.
- Jeong, A., Wong, M., 2015. Targeting the mammalian target of rapamycin for epileptic encephalopathies and malformations of cortical development. *J. Child Neurol.* 33, 55–63.
- Jin, Y.P., Valenzuela, N.M., Ziegler, M.E., Rozengurt, E., Reed, E.F., 2014. Everolimus inhibits anti-HLA I antibody-mediated endothelial cell signaling, migration and proliferation more potently than sirolimus. *Am. J. Transplant.* 14, 806–819.
- Jozwiak, S., Kotulska-Jozwiak, K., Bebin, M., Wong, M., 2020. Modifying Genetic Epilepsies – Results from Studies on Tuberous Sclerosis Complex and Their Potential Impact. *Neuropharmacology in press*.
- Kilkenny, C., Browne, W.J., Cuthill, I.C., Emerson, M., Altman, D.G., 2010. Improving bioscience research reporting: the ARRIVE guidelines for reporting animal research. *PLoS Biol.* 8, e1000412.
- Klawitter, J., Nashan, B., Christians, U., 2015. Everolimus and sirolimus in transplantation - related but different. *Expert Opin. Drug Saf.* 14, 1055–1070.
- Laplane, M., Sabatini, D.M., 2012. mTOR signaling in growth control and disease. *Cell* 149, 274–293.
- Leach, J.P., 2018. Treatment of Epilepsy - towards Precision, vol. 7, p. F1000Res.
- Lechuga, L., Franz, D.N., 2019. Everolimus as adjunctive therapy for tuberous sclerosis complex-associated partial-onset seizures. *Expert Rev. Neurother.* 19, 913–925.
- Lipton, J.O., Sahin, M., 2014. The neurology of mTOR. *Neuron* 84, 275–291.
- Lopes, M.W., Soares, F.M., de Mello, N., Nunes, J.C., de Cordova, F.M., Walz, R., Leal, R. B., 2012. Time-dependent modulation of mitogen activated protein kinases and AKT in rat hippocampus and cortex in the pilocarpine model of epilepsy. *Neurochem. Res.* 37, 1868–1878.
- Löscher, W., Ferland, R.J., Ferraro, T.N., 2017. The relevance of inter- and intrasrain differences in mice and rats and their implications for models of seizures and epilepsy. *Epilepsy Behav.* 73, 214–235.
- Löscher, W., Friedman, A., 2020. Structural, molecular and functional alterations of the blood-brain barrier during epileptogenesis and epilepsy: a cause, consequence or both? *Int. J. Mol. Sci.* 21, 591.
- Löscher, W., Potschka, H., Sisodiya, S.M., Vezzani, A., 2020. Drug resistance in epilepsy: clinical impact, potential mechanisms, and new innovative treatment options. *Pharmacol. Rev.* 72, 606–638.
- Maroso, M., Balosso, S., Ravizza, T., Iori, V., Wright, C.I., French, J., Vezzani, A., 2011. Interleukin-1beta biosynthesis inhibition reduces acute seizures and drug resistant chronic epileptic activity in mice. *Neurotherapeutics* 8, 304–315.
- Meikle, L., Pollizzi, K., Egnor, A., Kramvis, I., Lane, H., Sahin, M., Kwiatkowski, D.J., 2008. Response of a neuronal model of tuberous sclerosis to mammalian target of rapamycin (mTOR) inhibitors: Effects on mTORC1 and Akt signaling lead to improved survival and function. *Neurobiol. Dis.* 28, 5422–5432.
- Ostendorf, A.P., Wong, M., 2015. mTOR inhibition in epilepsy: rationale and clinical perspectives. *CNS Drugs* 29, 91–99.
- Paxinos, G., Franklin, K.B.J., 2012. In: Paxinos, G., Franklin, K.B.J. (Eds.), *The Mouse Brain in Stereotaxic Coordinates*, fourth ed. Academic Press, New York.
- Rageot, D., Bohnacker, T., Melone, A., Langlois, J.B., Borsari, C., Hillmann, P., Sele, A.M., Beaufils, F., Zvelebil, M., Hebeisen, P., Löscher, W., Burke, J., Fabbro, D., Wymann, M.P., 2018. Discovery and preclinical characterization of 5-[4,6-Bis(3-oxa-8-azabicyclo[3.2.1]octan-8-yl)-1,3,5-triazin-2-yl]-4-(difluoro methyl)pyridin-2-amine (PQR620), a highly potent and selective mTORC1/2 inhibitor for cancer and neurological disorders. *J. Med. Chem.* 61, 10084–10105.
- Rageot, D., Bohnacker, T., Keles, E., McPhail, J.A., Hoffmann, R.M., Melone, A., Borsari, C., Sriramaratnam, R., Sele, A.M., Beaufils, F., Hebeisen, P., Fabbro, D., Hillmann, P., Burke, J.E., Wymann, M.P., 2019. (S)-4-(Difluoromethyl)-5-(4-(3-methylmorpholino)-6-morpholino-1,3,5-triazin-2-yl) pyridin-2-amine (PQR530), a potent, orally bioavailable, and brain-penetrable dual inhibitor of class I PI3K and mTOR kinase. *J. Med. Chem.* 62, 6241–6261.
- Riban, V., Bouillieret, V., Pham, L., Fritschy, J.M., Marescaux, C., Depaulis, A., 2002. Evolution of hippocampal epileptic activity during the development of hippocampal sclerosis in a mouse model of temporal lobe epilepsy. *Neuroscience* 112, 101–111.
- Rogawski, M.A., Löscher, W., Rho, J.M., 2016. Mechanisms of action of antiseizure drugs and the ketogenic diet. *Cold Spring Harb. Perspect. Med.* 6, a022780.
- Saxton, R.A., Sabatini, D.M., 2017. mTOR signaling in growth, metabolism, and disease. *Cell* 168, 960–976.
- Shima, A., Nitta, N., Suzuki, F., Laharie, A.M., Nozaki, K., Depaulis, A., 2015. Activation of mTOR signaling pathway is secondary to neuronal excitability in a mouse model of mesio-temporal lobe epilepsy. *Eur. J. Neurosci.* 41, 976–988.
- Suzuki, F., Junier, M.P., Guilhem, D., Sorensen, J.C., Onteniente, B., 1995. Morphogenetic effect of kainate on adult hippocampal neurons associated with a prolonged expression of brain-derived neurotrophic factor. *Neuroscience* 64, 665–674.
- Switon, K., Kotulska, K., Janusz-Kaminska, A., Zmorzynska, J., Jaworski, J., 2017. Molecular neurobiology of mTOR. *Neuroscience* 341, 112–153.
- Talos, D.M., Jacobs, L.M., Gourmaud, S., Coto, C.A., Sun, H., Lim, K.C., Lucas, T.H., Davis, K.A., Martinez-Lage, M., Jensen, F.E., 2018. Mechanistic target of rapamycin complex 1 and 2 in human temporal lobe epilepsy. *Ann. Neurol.* 83, 311–327.
- Twele, F., Töllner, K., Brandt, C., Löscher, W., 2016a. Significant effects of sex, strain, and anesthesia in the intrahippocampal kainate mouse model of mesial temporal lobe epilepsy. *Epilepsy Behav.* 55, 47–56.
- Twele, F., Töllner, K., Bankstahl, M., Löscher, W., 2016b. The effects of carbamazepine in the intrahippocampal kainate model of temporal lobe epilepsy depend on seizure definition and mouse strain. *Epilepsia Open* 1, 45–60.
- Twele, F., Schidlitzki, A., Töllner, K., Löscher, W., 2017. The intrahippocampal kainate mouse model of mesial temporal lobe epilepsy: lack of electrographic seizure-like events in sham controls. *Epilepsia Open* 2, 180–187.
- Uhlmann, E.J., Wong, M., Baldwin, R.L., Bajenaru, M.L., Onda, H., Kwiatkowski, D.J., Yamada, K., Gutmann, D.H., 2002. Astrocyte-specific TSC1 conditional knockout

- mice exhibit abnormal neuronal organization and seizures. *Ann. Neurol.* 52, 285–296.
- van Vliet, E.A., Aronica, E., Gorter, J.A., 2015. Blood-brain barrier dysfunction, seizures and epilepsy. *Semin. Cell Dev. Biol.* 38, 26–34.
- Vezzani, A., 2012. Before epilepsy unfolds: finding the epileptogenesis switch. *Nat. Med.* 18, 1626–1627.
- Wicki, A., Brown, N., Xyrafas, A., Bize, V., Hawle, H., Berardi, S., Cmiljanovic, N., Cmiljanovic, V., Stumm, M., Dimitrijevic, S., Herrmann, R., Pretre, V., Ritschard, R., Tzankov, A., Hess, V., Childs, A., Hierro, C., Rodon, J., Hess, D., Joerger, M., von Moos, R., Sessa, C., Kristeleit, R., 2018. First-in human, phase 1, dose-escalation pharmacokinetic and pharmacodynamic study of the oral dual PI3K and mTORC1/2 inhibitor PQR309 in patients with advanced solid tumors (SAKK 67/13). *Eur. J. Canc.* 96, 6–16.
- Wong, M., 2013. Mammalian target of rapamycin (mTOR) pathways in neurological diseases. *Biomed. J.* 36, 40–50.
- Xu, C., Liu, C., Liu, L., Zhang, R., Zhang, H., Chen, S., Luo, Y., Chen, L., Huang, S., 2015. Rapamycin prevents cadmium-induced neuronal cell death via targeting both mTORC1 and mTORC2 pathways. *Neuropharmacology* 97, 35–45.
- Yang, M.T., Lin, Y.C., Ho, W.H., Liu, C.L., Lee, W.T., 2017. Everolimus is better than rapamycin in attenuating neuroinflammation in kainic acid-induced seizures. *J. Neuroinflammation* 14, 15.
- Zeng, L.H., Xu, L., Gutmann, D.H., Wong, M., 2008. Rapamycin prevents epilepsy in a mouse model of tuberous sclerosis complex. *Ann. Neurol.* 63, 444–453.